Nuclear Engineering and Technology 50 (2018) 1112–1119

Contents lists available at ScienceDirect

Nuclear Engineering and Technology

journal homepage: www.elsevier.com/locate/net

Original Article

Highly efficient adsorptive removal of uranyl ions from aqueous solutions using dicalcium phosphate nanoparticles as a superabsorbent

Hadis Saghatchi [a], Reza Ansari [a, b, *], H. Zavvar Mousavi [c]

[a] Department of Chemistry, Faculty of Science, University of Guilan, P.O. Box 41335-1914, Rasht, Iran
[b] The Caspian Sea Basin Research Center, University of Guilan, Rasht, 41996-13769, Iran
[c] Department of Chemistry, College of Science, Semnan University, Semnan, Iran

ARTICLE INFO

Article history:
Received 24 January 2018
Received in revised form
3 June 2018
Accepted 4 June 2018
Available online 5 June 2018

Keywords:
Uranium (VI)
Monetite
Nanoparticles
Adsorption
Adsorption isotherm

ABSTRACT

Dicalcium phosphate nanoparticles (DCP-NPs) was synthesized chemically and used for adsorptive removal of uranyl ions from aqueous solutions in a batch system. A commercial grade of DCP (monetite) was also employed for comparison. The synthesized and commercial adsorbents (S-DCP and C-DCP) were characterized by FT-IR, SEM and XRD techniques. The investigation of adsorption isotherms indicated that the maximum adsorption capacities (q_m) for C-DCP and S-DCP were 714.3 and 666.7 mg g^{-1} (at 293 K), respectively. The experimental kinetics were well-described by the pseudo-second-order kinetic and the equilibrium data were fitted with both Langmuir and Freundlich adsorption models. Thermodynamic studies indicated that the adsorption of uranyl ions on the monetite surface was a spontaneous exothermic process. The exhausted adsorbents could be regenerated by washing with 0.10 mol L^{-1} NaOH.

1. Introduction

Among the various heavy metals, uranium is one of the most dangerous for humans due to its toxicity and chemical radioactivity [1]. It enters into the water bodies through mining and milling procedures, applications of phosphate fertilizers to soils and the development of nuclear industries [2,3]. Uranium appears in the oxidation states of +2, +3, +4, +5 and + 6 in the nature, but the most common and stable oxidation states for this heavy metal are the tetravalent and hexavalent states which exist in acidic aqueous solutions as the linear uranyl ion $-UO_2^{2+}$-. Uranium (IV) is not soluble in water and usually precipitates, while uranium (VI) forms soluble ions, thus, it can be ingested and cause serious risks for human beings [4]. Uranyl ions can be retained in some body parts such as lung, bone, kidneys and liver and caused several health problems, including renal damage and different cancers [5]. Therefore, recently, several techniques have been tested for the removal of uranyl ions from aqueous solutions, including chemical precipitation [6], co-precipitation [7], solvent extraction [8], membrane dialysis [9], chromatographic extraction [10], ion exchange [11], flotation [12], and adsorption [13–19]. Compared to the other preceding methods which are expensive and time-consuming, adsorption is a low-cost method. It is also the most efficient method in terms of simplicity and feasibility with high potential for the removal, recovery and recycling of metal ions like uranyl from wastewaters [20–22].

Several studies about the application of the adsorption method for uranyl ion removal from aqueous solutions by various adsorbents are reported. Until now, the uranyl ion adsorption capacities of graphene oxide nanosheets [1], some pure and modified clays [23], Penicillium citrinum [24], magnetic chitosan [15], carboxyl-mesoporous carbon [25] surface modified magnetic Fe_3O_4 particles [26], melanin [27], and polymeric materials [28] have been evaluated. These studies revealed that adsorption process strongly depends on adsorbents characteristics and solution properties. Although these adsorbents provide some advantages, some of them are expensive. Hence, the aim of this research is to obtain low-cost and environmentally benign adsorbents [29–31].

Recently different minerals have been reported to remove uranyl ions from water resources [23,32]. Among them, those containing phosphate groups are more effective due to the formation of

* Corresponding author. Department of Chemistry, Faculty of Science, University of Guilan, P.O. Box 41335-1914, Rasht, Iran.
E-mail address: ransari271@guilan.ac.ir (R. Ansari).

https://doi.org/10.1016/j.net.2018.06.004

stable uranyl-phosphates crystalline structures [33]. A devious sign of the relationship between uranyl ions and phosphate was also been detailed by Abu-Hilal [34]. A lichen, Peltigera, has been used to take up uranyl ions with internal inorganic phosphate to create uranyl-phosphate crystals [35]. Citrobacter, a genus of Gram-negative coliform bacteria in the Enterobacteriaceae family, precipitates uranyl ions on its surfaces as uranyl phosphates [36].

Among the more common candidates in this regard, nano dicalcium phosphate anyhydrate (NDCPA, monetite, $CaHPO_4$), due to having phosphate groups, high surface area, avoiding pollutant release into the environment and low cost was chosen as adsorbent for uranyl removal. NDCP is one of the most stable phases of the dicalcium phosphates, which have attracted considerable attention. Lately, some researchers used monetite as an adsorbent for purification of aqueous solutions. Adsorption of malathion from aqueous solutions on monetite [37] and efficient removal of fluoride from drinking water using well-dispersed monetite bundles has also been reported recently [38].

In this work, adsorption of uranyl ions on the synthesized nano monetite particles was studied and the effect of the principle factors including pH, adsorbent dosage, contact time, initial concentration, ion Strength and desorption was evaluated for significant removal of uranyl ions from the aqueous solution. The adsorption kinetics, isotherms, thermodynamics and regeneration of the adsorbents have also been investigated. Finally, the uranyl ions adsorption performance of nano monetite particles was also compared with a commercial grade monetite (C-DCP) which can be used as a feed supplement in the Poultry industry.

2. Experimental

2.1. Materials and methods

All chemicals were of analytical grade reagent. A stock standard solution was prepared by dissolving an accurately weighed amount of $UO_2(NO_3)_2{\cdot}6H_2O$ (Fluka) in distilled water to yield 500 mg L^{-1} of uranyl ion. Various concentrations of uranyl ion from 10 to 400 mg L^{-1} were prepared by subsequent dilution of the stock solution. Arsenazo (III) used for spectrophotometric determination of uranyl ions was obtained from Aldrich.

The initial pH of the working solutions was adjusted by addition of HCl or NaOH solution. Hydrochloric acid, sodium hydroxide, calcium oxide, orthophosphoric acid solution and absolute ethanol were purchased from Merck. Double distilled water was used to prepare all the solutions.

2.2. Determination of uranium contents in the solution and procedure

A simple and sensitive spectrophotometric method based on colored complexes with Arsenazo (III) in aqueous medium was used for the determination of uranyl ions [39]. Known amounts of the standard solutions were placed in a 10 mL volumetric flask and completed to the final volume with double distilled water. The final concentrations of these solutions varied between 1.00-10.00 mg L^{-1} versus to uranyl ions. The calibration curve was constructed with several points as absorbance versus different uranium concentrations. The uranyl ions react with the Arsenazo (III) ions (0.10 g L^{-1}) to produce the blue-violet complex. The absorbance was measured at 650 nm against a blank for uranyl ion. The linear regression equation obtained from the calibration curve was $A = 0.0741\ C_{U(VI)}$ - 0.0086 ($R^2 = 0.9987$) in the concentration range of 1.00–10.00 mg L^{-1}. Beer's law is obeyed over the concentration range of 1.00–10.00 μg g^{-1} with a detection limit of 0.025 μg g^{-1}.

2.3. Preparation of nano monetite (NDCPA)

In a successful synthesis procedure to yield only single-phase monetite, 100 mL of ethanol was first placed into a 100 mL pyrex media bottle containing a Teflon-coated magnetic stir bar. 1.657 g of CaO powder (0.0296 mol Ca) was added into ethanol and the formed opaque suspension was magnetically stirred at room temperature for 5 min. Finally, 4 mL of H_3PO_4 (0.0592 mol P) was added into the calcite suspension, the glass bottle was tightly capped and the bottle contents were stirred at room temperature for 3 h. At the end of 3 h, the bottle was opened; the precipitates were filtered (Whatman No. 42 paper) and washed with 25 mL of ethanol. The precipitates was finally dried overnight at 37 °C in a static air oven [40].

2.4. Batch adsorption

Using a batch system, the effects of experimental factors such as pH, initial concentration, contact time, salt concentration and temperature were optimized in order to acquire the maximum adsorption. The pH was studied first in order to find out the maximum removal efficiency. The pH values were measured by a Denver digital pH meter during the experiments. In order to study the effect of adsorbent dosage, 25.0 mL of uranyl solutions (400 mg/L) were mixed with different dose of adsorbents (10.0–30.0 mg) at pH = 5, and room temperature for duration of 30 min. In order to find out the equilibrium time, fixed amounts(15.0 mg) of the employed adsorbents were mixed with uranyl solutions at room temperature at various exposure times (5–45 min) accompanied by shaking (250 rpm). For adsorption isotherm investigation, aliquots of 50 mL of uranyl solutions with various initial concentrations (10–500 mg/L) were agitated separately for duration of 30 min at room temperature. Thermodynamics studies were carried out by mixing adsorbents (10.0 mg) with uranyl solutions (50.0 mL) with initial concentration of 150 mg/L at three different temperatures (278, 298, 318, and 323 K). The contact time was kept as 30.0 min. When the adsorption process completed, the adsorbents were removed from the solution by filtration through a filter paper. The concentration of the adsorbed uranyl ions was determined from the difference between the initial and final concentrations of uranium in aqueous solution using a model Perlkin-Elmber Lambda EZ 201 UV-Vis spectrophotometer. Each experiment was repeated three times and the reported results are the average of these values. The following expressions were used to calculate the sorption percentage and sorption capacity (q_e). The special expressions were as Eq. (1, 2):

$$\%Sorption = \frac{C_0 - C_{eq}}{C_0} \times 100 \quad (1)$$

$$q_e = \frac{C_0 - C_{eq}}{m} \times V \quad (2)$$

where C_0 and C_{eq} are the liquid-phase concentrations of uranyl ions at initial and equilibrium time, respectively; m is the mass of the adsorbents (m), V is the volume of the suspension (L) and q_e (mg g^{-1}) is the amount of adsorbed uranyl ions on the adsorbents.

3. Results and discussion

3.1. Characterization of adsorbents

The FT-IR spectrum of monetite powder before and after uranyl ion adsorption is represented in Fig. 1. Fig. 1 a shows the spectrum of monetite. As can be seen in this figure, the band that occurs at

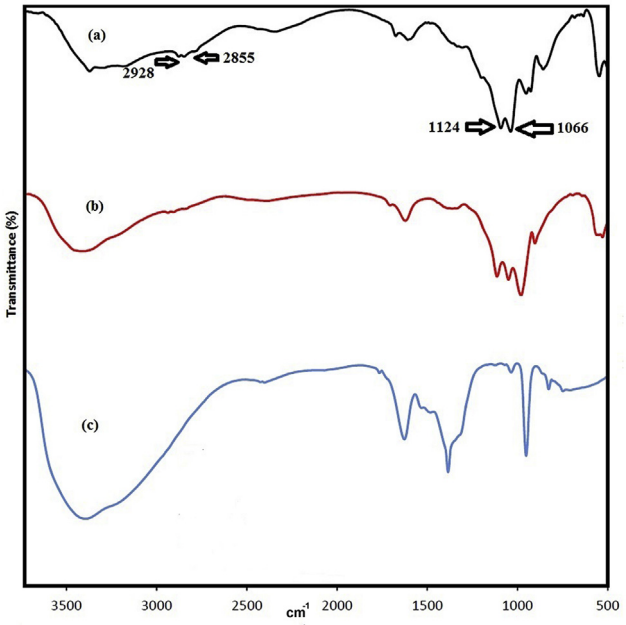

Fig. 1. The FT-IR pattern of (a) S-DCP before adsorption, (b) Uranium nitrate, (c) S-DCP after adsorption uranyl ions.

3437 cm^{-1} belongs to O–H stretching vibration of residual free water. Bands around 2928 and 2855 cm^{-1} correspond to (P) O–H stretching mode. The band at 1628 cm^{-1} belongs to H–O–H bending vibration mode. The bands of around 1124 and 1066 cm^{-1} are due to P–O stretching mode, and the band at 891 cm^{-1} belongs to P–O(H) stretching vibration mode. The band of around 570 cm^{-1} belongs to O–P–O(H) bending mode. These observations indicate that all the corresponding bands of monetite are present in its spectrum and confirm that monetite has been synthesized successfully [41,42]. Fig. 1b shows FT-IR spectrum of uranium nitrate and FT-IR spectrum of monetite after uranyl ion adsorption is shown in Fig. 1c. As it can be seen (Fig. 1b) after adsorption of uranyl ions, some decrease in the intensity of the characteristic peaks of monetite, attributed to P-O stretching (1066 and 1124 cm^{-1}), and also the peaks attributed to (P)O–H stretching (2928 and 2855 cm^{-1}), indicate that the phosphate groups are the main active sites for uptake of uranyl ions onto monetite [43,44].

The representative XRD pattern of monetite is shown in the inset of Fig. 2. The observed positions of diffraction lines were in agreement with the corresponding values for monetite ($CaHPO_4$, JCPD 09–0080). Monetite was identified by the appearance of well-defined peaks at the 2Θ angles of 13.1°, 26.4°, 26.6° and 30.2° [45].

Fig. 3 displayed the SEM images of nano monetite powders

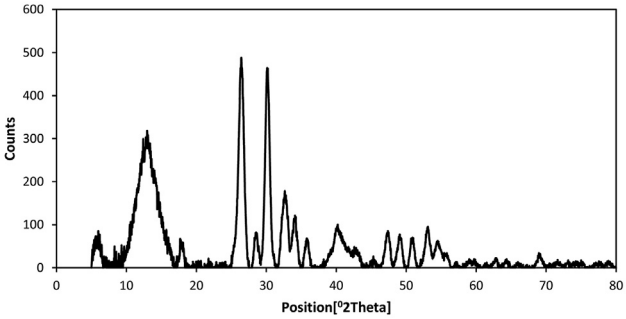

Fig. 2. XRD pattern of S-DCP.

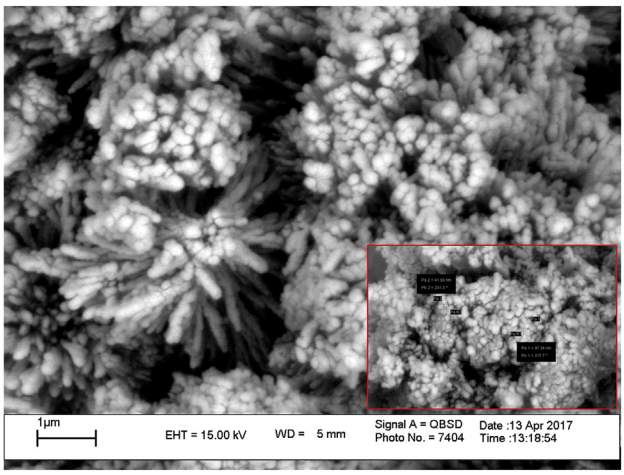

Fig. 3. The SEM image of NPs of S-DCP.

produced in 100 mL absolute EtOH using 0.0296 mol of precipitated CaO powder and 0.0592 mol H_3PO_4 as the starting materials. Especially, the inset of Fig. 3 clearly exhibited the nanoparticles of monetite stacked together to form the spherical particles. The average particle size was found to be in the range of 40–90 nm.

3.2. Studies of optimal conditions

3.2.1. Immersion technique for determination of pH_{pzc}

Suspensions of 10.0 g/L of monetite powder were put into contact with 0.010 mol L^{-1} NaCl solutions adjusted at different pH values from 2.0 to 11.0 using dilute HCl or NaOH solutions (0.10 mol L^{-1}). Then, they were agitated using a shaker at a speed of 250 rpm until an equilibrium pH value was reached. As shown in Fig. 4, the change of pH (ΔpH) during equilibration was calculated and the pH_{pzc} was identified as the initial pH with minimum ΔpH [46].

3.2.2. Effect of pH on uranyl adsorption

The adsorption of uranyl ions on the studied adsorbent as a function of pH is shown in Fig. 5. Monetite showed good uptake over a broad pH range. The maximum removal was observed in the pH range 3.0–7.0. As the results show, the pH dependence for C-DCP and S-DCP is different from each other. However, in pH range of 3.0–7.0, the differences are not considerable. The removal percentages for C-DCP are nearly constant from pH = 3 to 10 except the case of pH = 2. On the other hand, S-DCP shows removal percentage

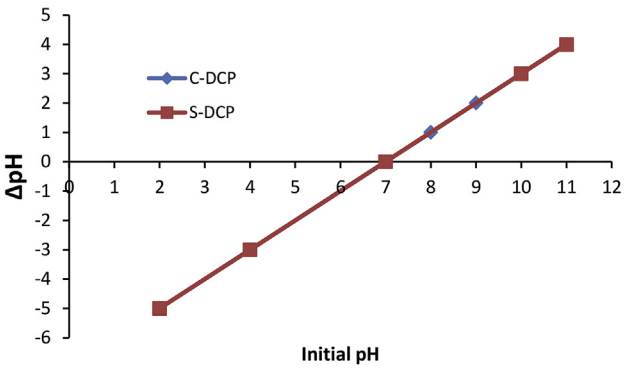

Fig. 4. Experimental immersion technique curves corresponding to monetite commercial and synthetic grades.

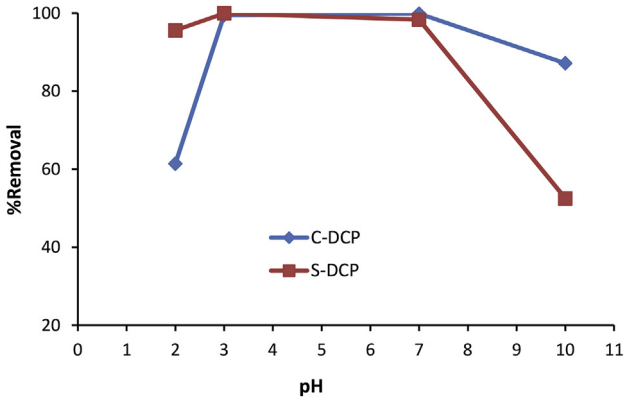

Fig. 5. The effect of the pH on uranyl ion sorption (m = 10.0 mg, V = 25 mL, T = RT, t = 30 min, C_0 = 200 mg L^{-1}, rpm = 250 min^{-1}, pH = 2–10).

at just pH = 10 are much lower than those at other pH cases.

The observed decrease in the uptake of the uranyl ions at pH > 7.0 can be explained on the basis of the formation of different uranyl species with lower adsorption affinities. At pH > 7.0, various oligomeric and monomeric hydrolyzed species of UO_2^{2+} are reported [15]. These include $[UO_2OH]^+$, $[(UO_2)_3(OH)_4]^{2+}$, $[(UO_2)_3(OH)_5]^+$, $[(UO_2)_2(OH)_2]^{2+}$, $[(UO_2)_2OH]^{3+}$, $[(UO_2)_3(OH)]^{5+}$, $[(UO_2)_4(OH)]^{7+}$, $[UO_2(OH)_4]^{2-}$, and $[(UO_2)_3(OH)_7]^-$. It was also reported that in the presence of carbonate anions monomeric and oligomeric carbonate species such as $[UO_2CO_3]^0$, $[UO_2(CO_3)_2]^{2-}$, $[UO_2(CO_3)_3]^{4-}$, and $[(UO_2)_3(CO_3)_6]^{6-}$ may also be formed. This dissolved carbonate and bicarbonate anions may form complex anions with uranyl ions, thus resulting in a decrease in the adsorption percentage [15,47]. In order to reasonably explain uranyl ion sorption behavior, the relative distributed proportion of uranyi ion species is illustrated in Fig. S1 [48].

Uptake of uranyl ions by monetite at neutral or acidic conditions may be explained via complex formation between uranyl ions and the phosphate groups on the monetite. As the pH decreases (pH < 3), the active sites (the phosphate groups) become protonated and their ability to interact with uranyl ions (UO_2^{2+}) is decreased. The points of zero charge (pzc) of both commercial dicalcium phosphate (C-DCP) and synthesized dicalcium phosphate (S-DCP) were found to be the same (pH_{pzc} = 7.0). At pH < 7, the positive zeta potential of the adsorbent indicates that the surface of the adsorbent becomes protonated. The negligible uptake of the uranyl ions on C-DCP and S-DCP at pH < 3.0 can be explained by the predominant electrostatic repulsion between the uranyl ions and the positively charged active sites of the adsorbents.

As reported (Fig. S1), at pH about 5, uranyl ions exist as positively charged species (mostly UO_2^{2+}) and unexpected removal increase, could be due to the high chemical affinity of uranyl ions to phosphate groups in monetite.

3.2.3. Effect of adsorbent doses

The effect of the adsorbent amount on the sorption of uranyl ions at C_0 = 400 mg L^{-1} was studied and the obtained results are shown in Fig. 6. The sorption percent of uranyl ions from solution obviously increased by increasing the adsorbent particles and then after that it remained constant. While, the adsorption capacity decreased with increasing the adsorbent dose (Fig. 6). The increase in sorption with an increase in the amount of adsorbent can be attributed to the availability of a larger surface area and more adsorption sites. With increasing adsorbent content, the available sites on the adsorbent surface increase and it provides more sorption sites to adsorb, and thereby results in the increase of the

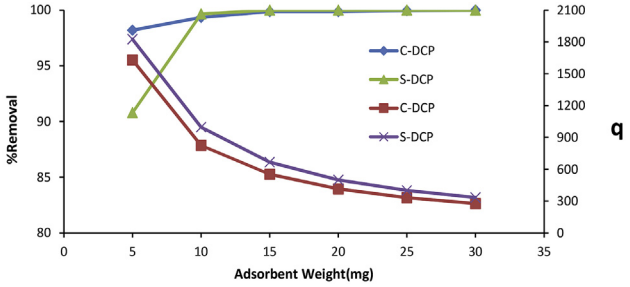

Fig. 6. Effect of the adsorbent amount on uranyl ion sorption by monetite and adsorption capacity. (pH = 5.0 ± 0.1, V = 25 mL, T = RT, t = 30 min, C_0 = 400 mg L^{-1}, rpm = 250 min^{-1}).

uranyl ions sorption. The decrease in the sorbent capacity may be due to interference between binding sites and higher adsorbed dose or deficiency of uranyl ions in the solution with respect to available binding sites [48].

3.2.4. Effect of contact time

Contact time is always can be considered as an important parameter in all of the sorption systems. Additionally, from studying this parameter, we can find out some important information such as sorption kinetics, sorption mechanism and also sorption capacity of an adsorbent. For this investigation, 15.0 mg of the adsorbents were agitated with 25 mL of uranyl test solutions with initial concentration of 200 mg/L for duration of various exposure times (5–45 min) at room temperature separately. The supernatant were analyzed for unabsorbed uranyl ions after each selected exposure time. The results obtained were presented in Fig. 7.

The amount of uranyl ion adsorbed per unit weight of the adsorbents was determined at certain periods of time (q_t). The uranyl ion adsorption increased with time and got equilibrium quickly within 10–15 min. A further increase in contact time has no effect on the uranyl ion adsorption. Although the equilibrium time was different for two adsorbents, it seems adsorption for both of them completed within 15 min. As shown (Fig. 7) S-DCP showed higher adsorption capacity toward uranyl ions compared to C-DCP. Achieving quick sorption equilibrium in the case of both adsorbents clearly implies that a great number of reaction active sites on monetite for uptake of uranyl ions are available.

3.2.5. Kinetic modeling

Kinetic modeling not only allows estimation of sorption rates, but also leads to suitable rate expressions characteristic of possible

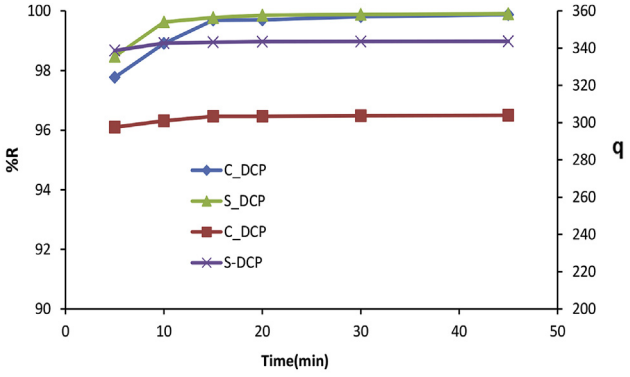

Fig. 7. Contact time effect on adsorption of uranyl ions and adsorption capacity (pH = 5.0 ± 0.1, V = 25 mL, C_0 = 200 mg L^{-1}, T = RT, rpm = 250 min^{-1}, m = 15.0 mg).

reaction mechanisms. In this respect, two kinetic models including the pseudo-first-order kinetics model and pseudo-second-order kinetics models were investigated. A pseudo-first-order kinetic equation is given by Eq. (3) [49]:

$$\ln(q_e - q_t) = \log q_e - \frac{k_1}{2.303} \times t \quad (3)$$

where q_t is the amount of uranyl ion adsorbed at time t (mg g^{-1}), q_e is the adsorption capacity at equilibrium (mg g^{-1}), k_1 is the pseudo-first-order rate constant (min^{-1}), and t is the contact time (min). Using Eq. (3), $ln(q_e - q_t)$ versus t can be plotted. In Pseudo-second-order model, the rate-limiting step is the surface adsorption that involves chemisorption, where the removal from a solution is due to physicochemical interactions between two phases. The pseudo-second-order kinetic equation is given by Eq. (4) [50]:

$$\frac{t}{q_t} = \frac{1}{k_2 q_e^2} + \frac{1}{q_e} \times t \quad (4)$$

where k_2 is the pseudo-second-order rate constant of adsorption [51]. The results obtained from the kinetics investigation are shown in Fig. S2. The kinetics parameters calculated, are summarized in Table 1.

Given that the correlation coefficients obtained for the pseudo-second-order model are obviously higher than the pseudo-first order model and the q_e value of this model is consistent with experimental results ($q_{e,exp}$). Therefore, it can be concluded that uranyl uptake using both of the applied adsorbents follows the pseudo-second-order model. The mechanism of the removal is chemisorption, involving valence forces through sharing or exchange of electron between the uranyl ions and the adsorbents [27,44].

3.2.6. Effect of the initial uranium concentration

The effect of the uranyl ion initial concentration on the adsorption rate was studied by contacting a fixed mass of adsorbent (20.0 mg) at room temperature (23 ± 2 °C) and pH (5.0 ± 0.1) using different concentrations of uranyl ion ranging from 10 to 500 mg L^{-1}. The results are given in Fig. 8. They reveal that the percentage of uranyl ion adsorption increased by decreasing the uranyl ion initial concentration, but it is not very sensitive to the uranyl ion concentration. In other words, the removal percentage of uranyl ion has been found to be favorably high in the studied concentration range. This tendency shows strong affinity of monetite toward uranyl ions, which seems phosphate groups are responsible for these strong interactions.

3.2.7. Adsorption isotherm studies

The adsorption data were analyzed with two sorption isotherms, namely Freundlich and Langmuir. The Langmuir model is characterized by an asymptotic shape while the Freundlich model supposes an exponential trend. The Freundlich equation predicts that the ion concentrations on the adsorbent will increase as long as there is an increase in the ion concentration in the liquid. The empirical model was shown to be consistent with an exponential distribution of active centers, characteristic of heterogeneous surfaces. The amount of solute adsorbed at equilibrium, q_e, is related to the concentration of solute in the solution, C_e, as Eq. (5):

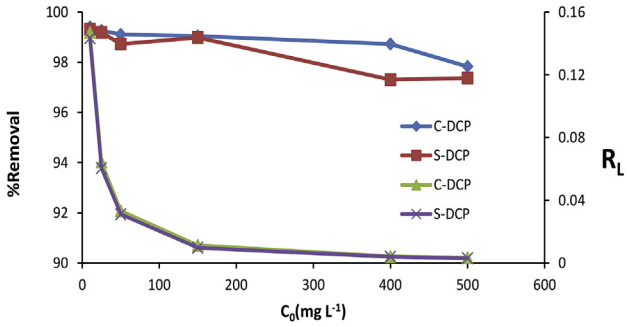

Fig. 8. Effect of initial uranium concentration on uranyl ion sorption and separation factor (R_L). C_0 = 10–500 mg L^{-1}, pH = 5.0 ± 0.1, T = RT, m = 20.0 mg, rpm = 250 min^{-1}, V = 50 mL, t = 30 min).

$$q_e = K_F C_e^{\frac{1}{n}} \quad (5)$$

This expression can be expressed by the Eq. (6):

$$\ln q_e = \ln K_F + \frac{1}{n} \ln c_e \quad (6)$$

where K_F and n are the Freundlich constants, which represent sorption capacity and sorption intensity, respectively. A plot of lnq_e versus lnc_e would result in a straight line with a slope of $1/n$ and intercept of log K_F as seen in Fig. S3a. Freundlich constants are given in Table 2. According to the Langmuir model, adsorption occurs uniformly on the active sites of the sorbent, and once a sorbate occupies a site, no further sorption can take place at this site. Thus, the Langmuir model is given by the Eq. (7):

$$\frac{1}{q_e} = \frac{1}{q_m} + \frac{1}{bq_m} \times \frac{1}{C_e} \quad (7)$$

where q_m and b, the Langmuir constants, are the saturated monolayer sorption capacity and the sorption equilibrium constant, respectively. A plot of $1/q_e$ versus $1/c_e$ would result in a straight line with a slope of $1/bq_m$ and intercept of $1/q_m$ as seen in Fig. S3b. The Langmuir parameters given in Table 2 can be used to predict the affinity between the sorbate and the sorbent using the dimensionless separation factor, R_L, expressed as in the following Eq. (8) [52].

Table 2
Isotherm constants and values of R^2.

Adsorbent	Langmuir isotherm			Freundlich isotherm		
	q_m (mg g^{-1})	b (L mg^{-1})	R^2	K_F (mg^{1+n}/g L^n)	n	R^2
C-DCP	714.28	0.58	0.995	242.25	1.24	0.9959
S-DCP	666.66	0.53	0.995	192.84	1.31	0.9958

Table 1
Pseudo-first and pseudo-second-order constants and values of R^2.

Adsorbent	Pseudo-first order				Pseudo-second order		
	$q_{e,exp}$(mg g^{-1})	$q_{e,cal}$ (mg g^{-1})	k_{1ads} (min^{-1})	R^2	$q_{e,cal}$ (mg g^{-1})	k_{2ads} (min^{-1})	R^2
C-DCP	303.38	9.44	3.1×10^{-1}	0.9013	303.03	3.6×10^{-2}	1
S-DCP	343.66	6.20	3.7×10^{-1}	0.9173	344.82	4.2×10^{-2}	1

$$R_L = \frac{1}{(1 + bC_0)} \quad (8)$$

The value of R_L indicates the type of isotherm to be irreversible if $R_L = 0$, favorable if $0<R_L < 1$, linear if $R_L = 1$ or unfavorable if $R_L > 1$. The values of R_L for adsorption of uranyl ions onto the both adsorbents are shown in Fig. 8. They indicate that the adsorption of uranyl ions on the adsorbents is more favorable at higher uranyl ion initial concentrations than at lower ones.

According to the experimental data for the adsorption of uranyl ions and the values of isotherm constants listed in Table 2, the adsorption of uranyl ions on the monetite surface follows both Langmuir and Freundlich adsorption isotherm. The obtained Langmuir monolayer adsorption capacity in the present study was found to be 714.3 and 666.7 mg g^{-1} (at 293 K) for C-DCP and S-DCP, respectively. Very well fitting of the Langmuir isotherm with the experimental data may be due to the homogeneous distribution of active sites on the adsorbent surface. Results show that monetite is efficient for the uranyl ion removal. The tendency of hexavalent uranyl ions to oxygen is high. Metal ions are classified by their binding favorites, specifically whether they look for O-, N-, or S-containing ligands. Pearson (1963) separated metal ions into the hard acids (O-seeking) and the soft acids (N- or S-seeking) [53]. Hard acids typically form complexes through carboxylate, carbonyl, alcohol, phosphate, and phosphodiester groups, while soft acids are predicted to bind to the sulfur sites, thioether, and amino groups. According to the theory of hard and soft acids and bases (HSAB) defined by Pearson, the oxygen-donor adsorption sites of the sorbents can be categorized as hard bases. These sites coordinate favorably with actinide ions ordered as hard acids. Uranyl ions could act as the hard acids and form strong complexes with oxygen-donor ligands existent in the phosphate groups of monetite. This phenomenon can enhance the efficiency of uranyl ions removal [44].

The q_m values of monetite are compared to those of different sorbents reported in the literature (Table 3). The monetite shows a high q_m (mg g^{-1}), which is higher than single-layered graphene oxide [1], zirconium-pillared clay [23], Penicillium citrinum [24], magnetic chitosan [15], carboxyl-mesoporous carbon [25], magnetic Fe_3O_4 [26], melanin [27], and polyaniline coated magnetic carboxymethylcellulose beads [28]. It is noteworthy that the affinity coefficient (b = 0.58–0.53 L/mg) was relatively higher for monetite compared to the above-mentioned sorbents. In the case of uranyl ion sorption, the comparison of q_m value of adsorbents used in the present study with that obtained in the literature shows that adsorbents used in the present study are more effective for this purpose.

Table 3
Maximum loading capacity of uranyl ion by different sorbents calculated from Langmuir adsorption isotherm.

Sorbent material	Uranyl ion sorption capacity (mg g^{-1})	References
Single-layered graphene oxide	299	[1]
Humic acid-immobilized zirconium-pillared clay	132.98	[23]
Penicillium citrinum	274.7	[24]
ion-imprinted magnetic chitosan resins	187	[15]
carboxyl-mesoporous carbon	250	[25]
surface modified magnetic Fe_3O_4 particles	151.80	[26]
Melanin	588.24	[27]
Polyaniline coated magnetic carboxymethylcellulose beads	386.5	[28]
Commercial monetite	*714.3*	*Present study*
Synthetic monetite	*666.7*	*Present study*

3.2.8. Thermodynamics studies

As shown in Fig. S4, the sorption of uranyl ions was investigated as a function of temperature. It can be seen that the removal percentage of uranyl ions increased with the increasing temperature, which suggested that the uranyl ions sorption process was favorable at higher temperature. The thermodynamic parameters obtained for the sorption process were calculated using Eq. (9):

$$\ln K_d = \frac{\Delta S^o_{ads}}{R} - \frac{\Delta H^o_{ads}}{RT} \quad (9)$$

where K_d is the distribution coefficient (mL g^{-1}), ΔS^o_{ads} is standard entropy (J mol^{-1} K^{-1}), ΔH^o_{ads} is standard enthalpy (kJ mol^{-1}), T is the absolute temperature (K), and R is the gas constant (8.314 J mol^{-1} K^{-1}) [52]. The experiments were carried out at 278, 298, 313 and 333 K for 100 mg L^{-1} uranyl ion solution. The values of ΔH^o_{ads} and ΔS^o_{ads} were calculated from the slopes and intercepts of the linear regression of lnK_D versus 1/T (inset of Fig. S4). The standard Gibbs free energy ΔG^o_{ads} values (kJ.mol^{-1}) were calculated from the Eq. (10):

$$\Delta G^o_{ads} = \Delta H^o_{ads} - T\Delta S^o_{ads} \quad (10)$$

The positive values of ΔH^o_{ads} indicated an endothermic adsorption process. The positive value of ΔS^o_{ads} indicated that the adsorption process was irreversible. In addition, the positive value of ΔS^o_{ads} is a favorable factor and the value of ΔH^o_{ads} that is lower than $|T\ \Delta S^o_{ads}|$ indicates that the adsorption process is dominated by entropic rather than enthalpy changes [54]. The values of ΔG^o_{ads} obtained at different temperatures are given in Table 4. The negative value of ΔG^o_{ads} indicated spontaneous nature of the adsorption process. On the other hand, the observed increase in the negative values of ΔG^o_{ads} with elevated temperature implies that the adsorption becomes more favorable at higher temperatures.

3.2.9. Effect of ionic strength

In this study, a series of experiments were carried out in various NaCl concentrations (from 0.10-0.70 M) in order to follow the effect of ionic strength. Aliquots of uranyl solutions (50 mL) with initial concentration of 200 mg/L were mixed with NaCl to fix the desired ionic strength. Then 10.0 mg of adsorbents were added. The mixtures were agitated at room temperature for duration 30 min. The results obtained are depicted in Fig. 9. As the results interestingly showed that removal of uranyl ion was not affected by the presence of NaCl. Generally, in sorption systems, removal via surface complexation is independent on ionic strength whereas is more dependent on the pH of the medium, whereas ion exchange is highly dependent on the ionic strength [5]. According to this, it could be concluded that the uranyl removal in the current work

Table 4
Thermodynamics parameters for adsorption of uranyl ions.

T (K)	K_d(mL/g)	ΔG^o_{ads} (kJ mol^{-1})	ΔS^o_{ads} (kJ mol^{-1} K^{-1})	ΔH^o_{ads}(kJ mol^{-1})
T-DCP				
278	114312.6	−26.62		
298	411571.4	−31.722	0.254	43.970
318	1116538	−36.802		
323	2798846	−40.612		
S-DCP				
278	110739.3	−26.63		
298	388513.5	−29.61	0.268	47.870
318	1343148	−34.81		
323	2075000	−38.71		

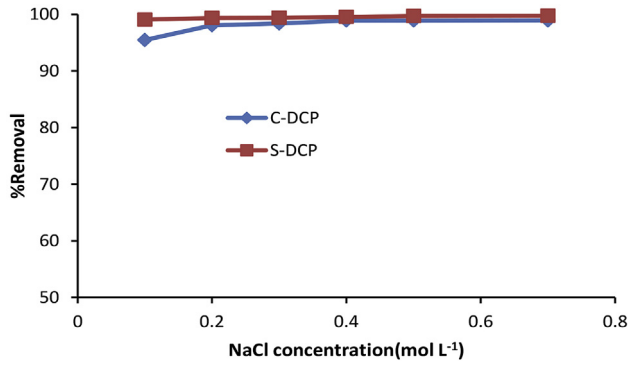

Fig. 9. Effect of NaCl concentration on uranyl ion sorption. (pH = 5.0, m = 10.0 mg, V = 50 mL, t = 30 min, C_0 = 200 mg L^{-1}, rpm = 250 min^{-1}).

involved the formation of a complex onto the adsorbent surface.

3.2.10. Desorption study

To evaluate the reusability of the adsorbents, 20.0 mL of 20 mg L^{-1} uranyl ion solution was first mixed with a fixed amount of the employed adsorbents and then the mixtures was shaken at room temperature for 30 min. The adsorbents were separated and the uranyl ion concentration in the supernatant was analyzed for remained or unadsorbed uranyl. In order to desorb the uranyl ions-loaded adsorbents, they were mixed with NaOH (0.10 M), ethanol and acetone as eluents. The mixtures were shaken for 30 min. Desorption percentage was calculated from the amount of uranyl ions adsorbed onto the adsorbents and the uranyl ions concentration in the eluent solution using equation (11):

$$\%Desorption = \frac{m}{m_0} \times 100 \quad (11)$$

where m is the amount of uranyl ion-desorbed (mg) and m_0 is the amount of uranyl ion-adsorbed (mg). Each adsorption and desorption experiment was carried out in triplicate and the average results are presented in this work. As indicate Table 5 desorption was observed only in the case of NaOH solution as eluent. Maximum desorption obtained was about 70% for both adsorbents. Due to high affinity of the DCP adsorbents toward uranyl ions, complete desorption cannot be achieved.

4. Conclusions

Here, monetite was synthesized chemically, characterized and then used as effective adsorbents for the removal of uranyl ions from aqueous solutions. Moreover, commercial monetite was purchased and used for the removal of uranyl ions. The maximum removal efficiency for both adsorbents was obtained at a broad range of pH (pH = 3–7), with the initial uranyl ions concentration of 200 mg L^{-1}. The isotherm analysis indicated that the equilibrium data were well fitted to both Langmuir model (R^2 = 0.9937) and Freundlich model (R^2= 0.9989). Furthermore, maximum adsorption capacity was found to be 714.3 and 666.7 mg g^{-1} (at 293 K) for C-DCP and S-DCP, respectively. The kinetic data were fitted to the pseudo-second-order model and the mechanism of adsorption was chemisorption. Thermodynamic studies depicted that the adsorption of uranyl ions on the monetite surface was exothermic and spontaneous. Desorption studies revealed that about 70% of the adsorbed uranyl ions could be desorbed with 0.10 mol L^{-1} NaOH solution obviously. Finally, comparison of two adsorbents with others lately studied adsorbents showed that monetite (dicalcium phosphate) can adsorb uranyl ions successfully due to having functional groups such as $-PO_4$ (phosphate) in its structure.

Table 5
Desorption using different eluents.

Elution solvent	DW[a]	Acetone	Ethanol	NaOH 0.10 M
%Desorption(S-DCP)	<2	<5	<5	**70.0**
%Desorption(C-DCP)	<2	<5	<5	**71.0**

[a] DW: Distilled Water.

Acknowledgements

The authors are grateful to University of Guilan and Caspian Sea Basin Research Center, University of Guilan for supporting of this work.

Appendix A. Supplementary data

Supplementary data related to this article can be found at https://doi.org/10.1016/j.net.2018.06.004.

References

[1] Z. Li, F. Chen, L. Yuan, Y. Liu, Y. Zhao, Z. Chai, W. Shi, Uranium (VI) adsorption on graphene oxide nanosheets from aqueous solutions, Chem. Eng. J. 210 (2012) 539–546.
[2] N. Yamaguchi, A. Kawasaki, I. Iiyama, Distribution of uranium in soil components of agricultural fields after long-term application of phosphate fertilizers, Sci. Total Environ. 407 (2009) 1383–1390.
[3] A. Krestou, A. Xenidis, D. Panias, Mechanism of aqueous uranium (VI) uptake by hydroxyapatite, Miner. Eng. 17 (2004) 373–381.
[4] R. Villalobos-Rodríguez, M. Montero-Cabrera, H. Esparza-Ponce, E. Herrera-Peraza, M. Ballinas-Casarrubias, Uranium removal from water using cellulose triacetate membranes added with activated carbon, Appl. Radiat. Isot. 70 (2012) 872–881.
[5] H.İ. Ulusoy, S. Şimşek, Removal of uranyl ions in aquatic mediums by using a new material: gallocyanine grafted hydrogel, J. Hazard. Mater. 254 (2013) 397–405.
[6] R. Ganesh, K.G. Robinson, L. Chu, D. Kucsmas, G.D. Reed, Reductive precipitation of uranium by Desulfovibrio desulfuricans: evaluation of cocontaminant effects and selective removal, Water Res. 33 (1999) 3447–3458.
[7] F.A. Aydin, M. Soylak, Solid phase extraction and preconcentration of uranium (VI) and thorium (IV) on Duolite XAD761 prior to their inductively coupled plasma mass spectrometric determination, Talanta 72 (2007) 187–192.
[8] M. Yaftian, R. Taheri, A. Zamani, D. Matt, Thermodynamics of the solvent extraction of thorium and europium nitrates by neutral phosphorylated ligands, J. Radioanal. Nucl. Chem. 262 (2004) 455–459.
[9] A. Kuhu, Electrochemistry of Cleaner Environments, Plenum Press, New York, 1972.
[10] M.L. Dietz, E.P. Horwitz, L.R. Sajdak, R. Chiarizia, An improved extraction chromatographic resin for the separation of uranium from acidic nitrate media, Talanta 54 (2001) 1173–1184.
[11] A.C.Q. Ladeira, C.A.d. Morais, Uranium recovery from industrial effluent by ion exchange—column experiments, Miner. Eng. 18 (2005) 1337–1340.
[12] T.P. Rao, P. Metilda, J.M. Gladis, Preconcentration techniques for uranium (VI) and thorium (IV) prior to analytical determination—an overview, Talanta 68 (2006) 1047–1064.
[13] K. Oshita, A. Sabarudin, T. Takayanagi, M. Oshima, S. Motomizu, Adsorption behavior of uranium (VI) and other ionic species on cross-linked chitosan resins modified with chelating moieties, Talanta 79 (2009) 1031–1035.
[14] M. Voronkov, N. Vlasova, Y.N. Pozhidaev, Organosilicon ion-exchange and complexing adsorbents, Appl. Organomet. Chem. 14 (2000) 287–303.
[15] L. Zhou, C. Shang, Z. Liu, G. Huang, A.A. Adesina, Selective adsorption of uranium (VI) from aqueous solutions using the ion-imprinted magnetic chitosan resins, J. Colloid Interface Sci. 366 (2012) 165–172.
[16] S. Nakamura, S. Mori, H. Yoshimuta, Y. Ito, M. Kanno, Uranium adsorption properties of hydrous titanium oxide granulated with polyacrylonitrile, Sep. Sci. Technol. 23 (1988) 731–743.
[17] K. Akiba, H. Hashimoto, Recovery of uranium by polyurethane foam impregnated with 5, 8-diethyl-7-hydroxy-6-dodecanone oxime, J. Radioanal. Nucl. Chem. 130 (1989) 13–20.
[18] Y. Liu, X. Cao, R. Hua, Y. Wang, Y. Liu, C. Pang, Y. Wang, Selective adsorption of uranyl ion on ion-imprinted chitosan/PVA cross-linked hydrogel, Hydrometallurgy 104 (2010) 150–155.
[19] S. Sadeghi, A.A. Mofrad, Synthesis of a new ion imprinted polymer material for separation and preconcentration of traces of uranyl ions, React. Funct. Polym. 67 (2007) 966–976.
[20] R. Donat, The removal of uranium (VI) from aqueous solutions onto natural

sepiolite, J. Chem. Thermodyn. 41 (2009) 829–835.
[21] R. Han, W. Zou, Y. Wang, L. Zhu, Removal of uranium (VI) from aqueous solutions by manganese oxide coated zeolite: discussion of adsorption isotherms and pH effect, J. Environ. J. Environ. Radioact. 93 (2007) 127–143.
[22] C. Jeon, J.Y. Park, Y.J. Yoo, Removal of heavy metals in plating wastewater using carboxylated alginic acid, Korean J. Chem. Eng. 18 (2001) 955–960.
[23] T. Anirudhan, C. Bringle, S. Rijith, Removal of uranium (VI) from aqueous solutions and nuclear industry effluents using humic acid-immobilized zirconium-pillared clay, J. Environ. Radioact. 101 (2010) 267–276.
[24] C. Pang, Y.-H. Liu, X.-H. Cao, M. Li, G.-L. Huang, R. Hua, C.-X. Wang, Y.-T. Liu, X.-F. An, Biosorption of uranium (VI) from aqueous solution by dead fungal biomass of Penicillium citrinum, Chem. Eng. J. 170 (2011) 1–6.
[25] Y.-Q. Wang, Z.-B. Zhang, Y.-H. Liu, X.-H. Cao, Y.-T. Liu, Q. Li, Adsorption of U (VI) from aqueous solution by the carboxyl-mesoporous carbon, Chem. Eng. J. l 198 (2012) 246–253.
[26] X. Zhang, J. Wang, R. Li, Q. Dai, L. Liu, Removal of uranium (vi) from aqueous solutions by surface modified magnetic Fe $_3$ O $_4$ particles, New J. Chem. 37 (2013) 3914–3919.
[27] A.S. Saini, J.S. Melo, Biosorption of uranium by melanin: kinetic, equilibrium and thermodynamic studies, Bioresour. Technol. 149 (2013) 155–162.
[28] M.Y. Arica, G. Bayramoglu, Polyaniline coated magnetic carboxymethylcellulose beads for selective removal of uranium ions from aqueous solution, J. Radioanal. Nucl. Chem. 310 (2016) 711–724.
[29] E. Pehlivan, T. Altun, S. Cetin, M.I. Bhanger, Lead sorption by waste biomass of hazelnut and almond shell, J. Hazard. Mater. 167 (2009) 1203–1208.
[30] D.H. Lee, H. Moon, Adsorption equilibrium of heavy metals on natural zeolites, Korean J. Chem. Eng. 18 (2001) 247–256.
[31] T.-Y. Kim, S.-K. Park, S.-Y. Cho, H.-B. Kim, Y. Kang, S.-D. Kim, S.-J. Kim, Adsorption of heavy metals by brewery biomass, Korean J. Chem. Eng. 22 (2005) 91–98.
[32] A. Jean, E. François, N. Joseph, A. Paola, N. Edouard, Batch experiments on the removal of U (VI) ions in aqueous solutions by adsorption onto a natural clay surface, J. Environ. Earth Sci. 3 (2013) 11–23.
[33] S. Raicevic, J. Wright, V. Veljkovic, J. Conca, Theoretical stability assessment of uranyl phosphates and apatites: selection of amendments for in situ remediation of uranium, Sci. Total Environ. 355 (2006) 13–24.
[34] A.H. Abu-Hilal, Effect of depositional environment and sources of pollution on uranium concentration in sediment, coral, algae and seagrass species from the Gulf of Aqaba (Red Sea), Marine Poll Bull 28 (1994) 81–88.
[35] J.R. Haas, E.H. Bailey, O.W. Purvis, Bioaccumulation of metals by lichens: uptake of aqueous uranium by Peltigera membranacea as a function of time and pH, Am. Mineral. 83 (1998) 1494–1502.
[36] M. Roig, T. Manzano, M. Diaz, Biochemical process for the removal of uranium from acid mine drainages, Water Res. 31 (1997) 2073–2083.
[37] M. Mirković, T.L. Pašti, A. Došen, M. Čebela, A. Rosić, B. Matović, B. Babić, Adsorption of malathion on mesoporous monetite obtained by mechanochemical treatment of brushite, RSC Adv. 6 (2016) 12219–12225.
[38] C. Shen, L. Wu, Y. Chen, S. Li, S. Rashid, Y. Gao, J. Liu, Efficient removal of fluoride from drinking water using well-dispersed monetite bundles inlaid in chitosan beads, Chem. Eng. J. 303 (2016) 391–400.
[39] P. Misaelides, A. Godelitsas, A. Filippidis, D. Charistos, I. Anousis, Thorium and uranium uptake by natural zeolitic materials, Sci. Total Environ. 173 (1995) 237–246.
[40] A.C. Tas, Monetite ($CaHPO_4$) synthesis in ethanol at room temperature, J. Am. Ceram. Soc. 92 (2009) 2907–2912.
[41] S. Baradaran, W. Basirun, M. Mahmoudian, M. Hamdi, Y. Alias, Synthesis and characterization of monetite prepared using a sonochemical method in a mixed solvent system of water/ethylene glycol/N, N-dimethylformamide, Metall. Mater. Trans. A 44 (2013) 2331–2338.
[42] E. Salimi, J. Javadpour, Synthesis and characterization of nanoporous monetite which can be applicable for drug Carrier, J. Nanomater 2012 (2012) 135.
[43] M. Sureshkumar, D. Das, M. Mallia, P. Gupta, Adsorption of uranium from aqueous solution using chitosan-tripolyphosphate (CTPP) beads, J. Hazard. Mater. 184 (2010) 65–72.
[44] L. Zhou, Z. Huang, T. Luo, Y. Jia, Z. Liu, A.A. Adesina, Biosorption of uranium (VI) from aqueous solution using phosphate-modified pine wood sawdust, J. Radioanal. Nucl. Chem. 303 (2015) 1917–1925.
[45] N.A. Medellin-Castillo, E. Padilla-Ortega, L.D. Tovar-García, R. Leyva-Ramos, R. Ocampo-Pérez, F. Carrasco-Marín, M.S. Berber-Mendoza, Removal of fluoride from aqueous solution using acid and thermally treated bone char, Adsorpt 22 (2016) 951–961.
[46] N. Fiol, I. Villaescusa, Determination of sorbent point zero charge: usefulness in sorption studies, Environ. Chem. Lett. 7 (2009) 79–84.
[47] W. Dong, S.C. Brooks, Determination of the formation constants of ternary complexes of uranyl and carbonate with alkaline earth metals (Mg^{2+}, Ca^{2+}, Sr^{2+}, and Ba^{2+}) using anion exchange method, Environ. Sci. Technol. 40 (2006) 4689–4695.
[48] P. Zong, S. Wang, Y. Zhao, H. Wang, H. Pan, C. He, Synthesis and application of magnetic graphene/iron oxides composite for the removal of U (VI) from aqueous solutions, Chem. Eng. J. 220 (2013) 45–52.
[49] J.-f. Liu, Z.-s. Zhao, G.-b. Jiang, Coating Fe_3O_4 magnetic nanoparticles with humic acid for high efficient removal of heavy metals in water, Environ. Sci. Technol. 42 (2008) 6949–6954.
[50] H. Wang, A. Zhou, F. Peng, H. Yu, J. Yang, Mechanism study on adsorption of acidified multiwalled carbon nanotubes to Pb (II), J. Colloid Interface Sci. 316 (2007) 277–283.
[51] D. Robati, Pseudo-second-order kinetic equations for modeling adsorption systems for removal of lead ions using multi-walled carbon nanotube, J. nanostructure chem. 3 (2013) 55.
[52] A. Mellah, S. Chegrouche, M. Barkat, The removal of uranium (VI) from aqueous solutions onto activated carbon: kinetic and thermodynamic investigations, J. Colloid Interface Sci. 296 (2006) 434–441.
[53] R.G. Pearson, Hard and soft acids and bases, JACS 85 (1963) 3533–3539.
[54] A.M. Donia, A.A. Atia, E.M. Moussa, A.M. El-Sherif, M.O.A. El-Magied, Removal of uranium (VI) from aqueous solutions using glycidyl methacrylate chelating resins, Hydrometallurgy 95 (2009) 183–189.